Author's Accepted Manuscript

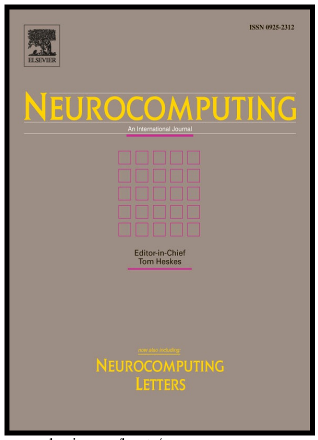

www.elsevier.com/locate/neucom

Adaptive RBFNNs/integral sliding mode control for a quadrotor aircraft

Shushuai Li, Yaonan Wang, Jianhao Tan, Yan Zheng

PII: S0925-2312(16)30778-0
DOI: http://dx.doi.org/10.1016/j.neucom.2016.07.033
Reference: NEUCOM17390

To appear in: *Neurocomputing*

Received date: 11 October 2015
Revised date: 20 May 2016
Accepted date: 17 July 2016

Cite this article as: Shushuai Li, Yaonan Wang, Jianhao Tan and Yan Zheng, Adaptive RBFNNs/integral sliding mode control for a quadrotor aircraf *Neurocomputing,* http://dx.doi.org/10.1016/j.neucom.2016.07.033

Adaptive RBFNNs/integral sliding mode control for a quadrotor aircraft

Shushuai Li*, Yaonan Wang, Jianhao Tan, Yan Zheng

College of Electrical and Information Engineering, Hunan University, Changsha Hunan, 410082, China

Abstract

This paper presents a novel hierarchical control strategy based on adaptive radical basis function neural networks (RBFNNs) and double-loop integral sliding mode control (IntSMC) for the position and attitude tracing of quadrotor unmanned aerial vehicles (UAVs) subjected to sustained disturbances and parameter uncertainties. The dynamical motion equations are obtained by the Lagrange-Euler formalism. The proposed controller combines the advantage of the IntSMC with the approximation ability of arbitrary functions ensured by RBFNNs to generate a control law to guarantee the faster convergence of the state variables to their desired values in short time and compensation for the disturbances and uncertainties. Capabilities of online adaptive estimating of the unknown uncertainties and null tracking error are proved by using the Lyapunov stability theory. Simulation results, also compared with traditional PD/IntSMC algorithms and with the backstepping/nonlinear H_∞ controller, verify the effectiveness and robustness of the proposed control laws.

Keywords: Quadrotor aircrafts, adaptive RBFNNs control, double-loop integral sliding mode control, hierarchical control

*Corresponding author.
Email address: shsli@hnu.edu.cn (Shushuai Li)

1. Introduction

Quadrotor UAVs have received increasing attentions in the past decade, because of their specific characteristics such as autonomous flight, low cost, vertical takeoff/landing ability and onboard vision system [1, 2], and their wide applications like surveillance, building exploration and information collection [3, 4]. However, trajectories tracking control of quadrotor UAVs is a major open problem as control strategy for fully actuated systems cannot be applied to underactuated quadrotor systems directly due to the six degrees of freedom (DOF) with only four control inputs [5]. And nonlinear coupled behavior complicates the control design stage even more. In addition, external disturbances and parameter uncertainties are ubiquitous phenomena in practical quadrotor aircrafts affected by wind gusts, payload, internal friction and model uncertainties. They should be explicitly considered in controller design; otherwise, the affected control inputs possibly lead to degraded performance and even instability of the closed loop. Thus, all these factors claim for a powerful, anti-disturbance, robust and intelligent control law for path following problems of small quadrotor aircrafts.

In the relevant literatures, different control strategies have been proposed to deal with path following problem of quadrotor systems. The linear control methods such as the application of proportional-integral-derivative (PID) control and linear-quadratic regulator to a quadrotor were presented in [6, 7]. In [8], a PD^2 controller was proposed and exponential convergence of tracking errors was attained. However, for these linear control techniques, the convergence can not be guaranteed when the vehicle moves away from its flight domain, and these control approaches have limited capability to alleviate the coupling among variables.

Moreover, since the nonlinear control methods can overcome some of the limitations and drawbacks of linear approaches by substantially expanding the domain of controllable flights, a variety of nonlinear flight control methods have also been developed. In [9], backstepping control was proposed and applied to nonlinear quadrotor systems, which guaranteed the asymptotic convergence of tracking errors. Researchers worked also on switching model predictive control (MPC) for attitude stabilization in [10] with respect to the induced wind disturbances, and [11] used support vector regression for predicting the future states in the MPC framework to control fixed-wing UAVs. An underactuated H_∞ control strategy was proposed in [12] to control the attitude and altitude of a helicopter, while outer-loop control was performed using a model-based predictive controller to track the reference trajectory. A fuzzy sliding mode control for keeping aircrafts following the predetermined trajectory was proposed, and the fuzzy inference mechanism helped to estimate the upper bound of lumped uncertainty [13]. Based on visual servo control, quadrotor UAVs used a nonhomogeneous gain term to reduce errors of visual sensitivity and accurate tracking of the target was realized [14]. Bounded errors in attitude and position tracking were guaranteed by a nonlinear robust tracking control strategy [15, 16]. Super twisting algorithm has been applied to a quadrotor in [17] in order to ensure robustness against bounded disturbances. Direct approximate-adaptive control composed of combined model adaptive control (CMAC) and nonlinear approximation has been proposed in [18], and robustness properties to unknown payloads and disturbances have been proved. In [19], active fault-tolerant control was applied to aircrafts by using the flatness concept, where both faults and saturation problem in actuators were handled effectively. As for multiple UAVs, artificial potential field method was introduced such that quadrotor UAVs can track the desired trajectory coordinately [20].

However, discontinuities caused by some robust control methods may be harmful for air nonlinear plants [21], and the backstepping approach usually requires full knowledge of dynamics, which stands for an extremely difficult assumption to meet in practice for UAVs [22]. To overcome the drawbacks of the existing control methods, this paper presents an innovative control scheme for robust convergence and disturbance attenuation of quadrotor position and attitude tracing. Adaptive RBFNNs control is introduced for the position tracking, estimating unknown model parameters and sustained perturbation during the whole operational process [23]. The tracking error is uniform ultimate bounded with the bound being adjustable, and the RBFNNs is trained online using an adaptive law based on Lyapunov approach and it offers the possibility of adaptation to any changes that can happen during the use of the system [24]. Moreover, given that the comprehensive nonlinear model of the UAV quadrotor attitude subsystem, double-loop IntSMC is designed to simplify the control law design, and attitude state variables restricted to the manifolds have a desired dynamics of asymptotic convergence and robustness properties in implementation. Besides, the integral action helps eliminate tracking errors even in the presence of disturbances and parametric uncertainties [25]. In order to eliminate the chattering phenomenon in sliding mode control, the sigmoid function is introduced to replace the sign function. Compared with the existing control algorithms in many publications, the main contributions of our proposed control algorithms are as follows: (i) this hierarchical control scheme offers superior properties such as faster convergence and higher precision than some nonlinear control methods, and it also has disturbance rejection capability and robustness against the model uncertainties, (ii) the tracking error reaches an ultimately bound around zero which can be made arbitrarily small by selecting appropriate control parameters, (iii) this method has larger control domain than that of linear approaches and continuous control signals promote the possibilities of this technique in real-time application.

The rest of this paper is organized as follows. In section 2, the tracing control problem of quadrotor aircrafts modeled by Lagrange-Euler formalism is presented. In section 3, the control scheme composed of an adaptive RBFNNs control for position tracing and a double-loop integral sliding mode control to stabilize aircrafts attitude is proposed. In section 4, simulation results are provided to demonstrate the effectiveness and robustness of the proposed methods. Finally, the conclusions of this paper are drawn in section 5.

2. The dynamic model of quadrotor

In this paper, we consider a quadrotor aircraft subjected to parameter uncertainties, aerodynamic drag and wind gusts. This kind of quadrotor aircraft can be modeled by Euler formalism. As shown in Figure 1, a quadrotor is a cross rigid frame with four rotors to produce the driving forces.

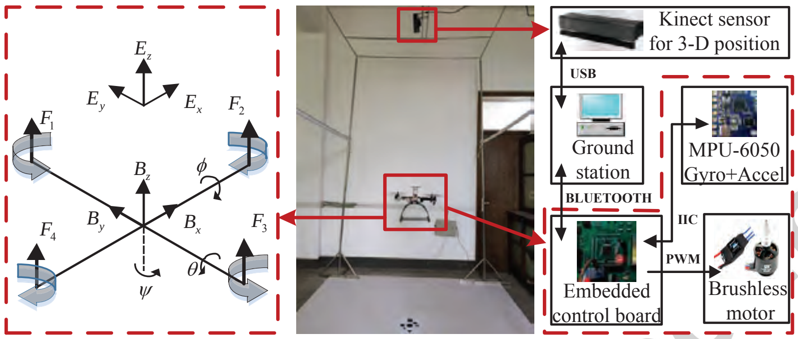

Figure 1. Quadrotor model.

In quadrotor systems, Ω_i stands for angular speed of the ith propeller. Based on simplified rotor model, we can use rotational speed $\Omega \in R^4$ to obtain control inputs T, τ_1, τ_2 and τ_3, defined as [8]

$$\begin{cases} T = b\sum_{i=1}^{4}\Omega_i^2 \\ \tau_1 = db(\Omega_1^2 - \Omega_3^2) \\ \tau_2 = db(\Omega_2^2 - \Omega_4^2) \\ \tau_3 = \kappa(\Omega_1^2 + \Omega_3^2 - \Omega_2^2 - \Omega_4^2), \end{cases} \tag{1}$$

where $T \in R$ is thrust magnitude, $\tau = [\tau_1, \tau_2, \tau_3]^T \in R^3$ are roll, pitch and yaw moments, d represents the distance from mass center to each rotor, $\kappa > 0$ and $b > 0$ are thrust and drag coefficients, respectively. Finally, thrust magnitude T and items of the moment vector τ are regarded as four control inputs of quadrotor aircraft systems.

Let $B = [B_x, B_y, B_z]$ be the body-frame coordinates shown in Figure 1, and let $E = [E_x, E_y, E_z]$ be the earth-frame coordinates. A quadrotor system has six state variables, three translational motion $\xi = [x, y, z]^T$ and three rotational motion $\eta = [\phi, \theta, \psi]^T$. By sequentially rotating aircrafts around the three axis in body coordinates, rotation matrix R_{BE} can be obtained to describe the linear velocity relationship between body-frame and inertial-frame [5]. The rotation matrix is given by

$$R_{BE} = \begin{bmatrix} C\psi C\theta & C\psi S\theta S\phi - S\psi C\phi & C\psi S\theta C\phi + S\psi S\phi \\ S\psi C\theta & S\psi S\theta S\phi + C\psi C\phi & S\psi S\theta C\phi - C\psi S\phi \\ -S\theta & C\theta S\phi & C\theta C\phi \end{bmatrix}, \tag{2}$$

where $C\bullet = cos(\bullet)$ and $S\bullet = sin(\bullet)$.

Matrix W_{BE} can be obtained to describe the angular velocity relationship between body-frame and inertial-frame [26], which is defined as

$$W_{BE} = \begin{bmatrix} 1 & sin\phi tan\theta & cos\phi tan\theta \\ 0 & cos\phi & -sin\phi \\ 0 & sin\phi sec\theta & cos\phi sec\theta \end{bmatrix}. \tag{3}$$

Let $q = [x, y, z, \phi, \theta, \psi]^T$ be state variables of quadrotors. The aircraft mathematical model can be defined with Lagrange-Euler equations

$$L(q, \dot{q}) = E_T + E_R - E_P, \tag{4}$$

$$\frac{\mathrm{d}}{\mathrm{dt}} \frac{\partial L}{\partial \dot{q}} - \frac{\partial L}{\partial q} = \begin{bmatrix} \zeta \\ \tau \end{bmatrix}, \tag{5}$$

where L is the Lagrangian of the model, $E_T = (m/2)\dot{\xi}^T \dot{\xi}$ is the translational kinetic energy, $E_R = (1/2)\dot{\omega}^T I \dot{\omega}$ is the rotational kinetic energy, ω is the angular velocity resolved in body-frame, I is the inertial matrix, $E_P = [0, 0, mgz]^T$ is the potential energy, m is the mass of the aircraft, g is the gravitational acceleration, and $\zeta = R_{BE}[0, 0, T]^T$ is the translational force due to thrust magnitude T.

According to (5), the aircraft model can be divided into two subsystems. For translational subsystem, model equation can be written as

$$m\ddot{\xi} + mg[0, 0, 1]^T = \zeta. \tag{6}$$

From (3), the angular velocity correlation is defined as follows

$$\dot{\eta} = W_{BE}\omega. \tag{7}$$

To represent the rotational energy E_R as a function of the generalized coordinate η, we substitute (7) into rotational energy equation E_R, and obtain the following equation

$$E_R = \frac{1}{2}\dot{\eta}^T {W_{BE}^{-1}}^T I W_{BE}^{-1}\dot{\eta}. \tag{8}$$

The model equation of rotational subsystem can be obtained from (4), (5) and (8), that is

$$M(\eta)\ddot{\eta} + C(\eta, \dot{\eta})\dot{\eta} = \tau, \tag{9}$$

where $M(\eta) = {W_{BE}^{-1}}^T I W_{BE}^{-1}$, and matrix $M(\eta)$ is written as

$$M(\eta) = \begin{bmatrix} I_{xx} & 0 & -I_{xx}S\theta \\ 0 & I_{yy}C^2\phi + I_{zz}S^2\phi & (I_{yy} - I_{zz})C\phi S\phi C\theta \\ -I_{xx}S\theta & (I_{yy} - I_{zz})C\phi S\phi C\theta & I_{xx}S^2\theta + I_{yy}S^2\phi C^2\theta + I_{zz}C^2\phi C^2\theta \end{bmatrix}. \tag{10}$$

Since the form of matrix $C(\eta, \dot{\eta})$ is complex, we have not given it here, and the specific expression can be found in [27].

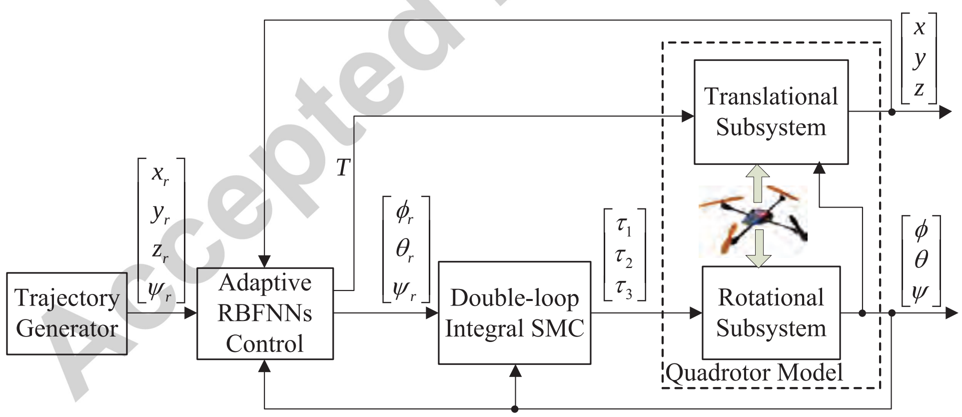

Figure 2. Control scheme.

Therefore, translational subsystem equation and rotational subsystem equation are given by (6) and (9) respectively. The objective of this paper is to design the control input signals of T and τ to guarantee the trajectory tracing for nonlinear coupling and underactuated quadrotors, rejecting the effect of the disturbance and parameter uncertainties. The overall control strategy is illustrated in Figure 2.

3. Controller Design

The overall control objective for the UAV is to track a desired trajectory $\xi_r = [x_r, y_r, z_r]^T$ and a desired yaw angle ψ_r. In translational subsystem, an adaptive RBFNN controller is designed to calculate T, ϕ_r and θ_r, which enables the aircraft to track the desired trajectory ξ_r, and neural network compensation helps eliminate the effects caused by parameter uncertainties and disturbances. Therefore, desired angles $\eta_r = [\phi_r, \theta_r, \psi_r]^T$ are derived. In rotational subsystem, an integral sliding mode controller is used to obtain proper values of rotor moment $\tau = [\tau_1, \tau_2, \tau_3]^T$ to make the aircraft track the desired attitude angles η_r, and the integral item helps eliminate state errors. Finally, stability analysis is proved by using Lyapunov theory.

3.1. Adaptive RBFNNs Control for Position Tracing

Translational dynamic equation is described in (6). To begin, define new control inputs u_1 and u_2, satisfying

$$\begin{cases} u_1(t) = cos\psi(t)sin\theta(t)cos\phi(t) + sin\psi(t)sin\phi(t) \\ u_2(t) = sin\psi(t)sin\theta(t)cos\phi(t) - cos\psi(t)sin\phi(t). \end{cases} \tag{11}$$

In view of (6), (11), parameter uncertainties and disturbances, the translational dynamics can be rewritten as follows

$$\ddot{\xi} + \Delta(\xi, \dot{\xi}, \ddot{\xi}) + D_\xi = \begin{bmatrix} 1/m & 0 & 0 \\ 0 & 1/m & 0 \\ 0 & 0 & cos\theta cos\phi/m \end{bmatrix} u - g \begin{bmatrix} 0 \\ 0 \\ 1 \end{bmatrix}, \tag{12}$$

where $\Delta(\xi, \dot{\xi}, \ddot{\xi}) \in R^3$ is the vector of model uncertainties, $D_\xi = [D_{\xi x}, D_{\xi y}, D_{\xi z}]^T$ is the disturbance force like wind, and $u = [u_1, u_2, T]^T$ is the control input.

The displacement tracking error can be defined as follows:

$$\widetilde{\xi}(t) = \xi_r(t) - \xi(t). \tag{13}$$

Assumption 3.1. *The real-time ξ and the desired ξ_r and its first-order derivative $\dot{\xi}_r$, and its second order derivative $\ddot{\xi}_r$ are all measurable.*

The following auxiliary state error vector $\gamma(t)$ is introduced to facilitate the control formulation and stability analysis:

$$\gamma(t) = \dot{\widetilde{\xi}}(t) + \Lambda\widetilde{\xi}(t), \tag{14}$$

where $\Lambda = \Lambda^T > 0$. Substituting the derivative of (13) into (14) reveals

$$\dot{\xi} = \dot{\xi}_r - \gamma + \Lambda\widetilde{\xi}. \tag{15}$$

Substituting (12) and (15) into the derivative of (14) leads to

$$\begin{aligned} \dot{\gamma} &= \ddot{\xi}_r - \ddot{\xi} + \Lambda\dot{\widetilde{\xi}} \\ &= \ddot{\xi}_r + \Lambda\dot{\widetilde{\xi}} - Mu + ge_3 + \Delta(\xi, \dot{\xi}, \ddot{\xi}) + D_\xi \\ &= -Mu + ge_3 + f, \end{aligned} \tag{16}$$

where M=diag$[1/m, 1/m, cos\theta cos\phi/m]$, $e_3 = [0, 0, 1]^T$, and $f = \ddot{\xi}_r + \Lambda\dot{\widetilde{\xi}} + \Delta(\xi, \dot{\xi}, \ddot{\xi}) + D_\xi$ represents the whole dynamic model including nominal model and unknown parts.

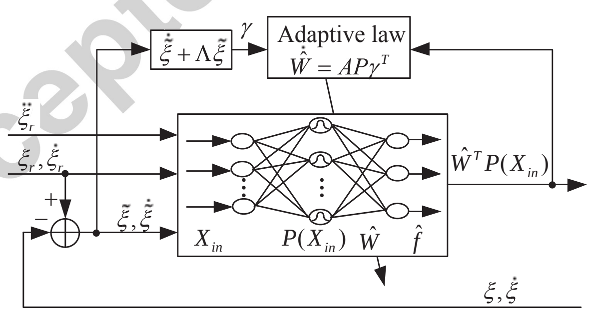

Figure 3. Adaptive RBFNNs control.

Adaptive RBFNNs scheme is proposed for the unknown MIMO nonlinear system, as RBFNNs can estimate the unknown continuous functions f and ensure tracking error ultimately converges to an adequately small compact set [28, 29]. Illustrated in Figure 3, the adaptive RBFNNs can be written as

$$\hat{f}(X_{in}) = \hat{W}^T P(X_{in}), \tag{17}$$

where $\hat{f} \in R^O$ is the NNs output vector, $X_{in} \in R^I$ is the input vector of the RBFNNs, $W \in R^{J\times O}$ is the weight vector, $J > 1$ is the nodes number of middle hidden layer, and $P(\bullet) : R^I \to R^J$ is the basis function vector with p_i being the commonly used Gaussian functions, which is simplified as

$$p_i(X_{in}) = \exp\left(-\frac{\|\mathrm{X_{in}} - \mathrm{c_i}\|^2}{\sigma_\mathrm{i}^2}\right), \tag{18}$$

where c_i is the center of the receptive field, and σ_i is the width of the Gaussian function. There exists an optimal vector W^* such that [30]

$$f(X_{in}) = W^{*T} P(X_{in}) + \epsilon, \tag{19}$$

where $\epsilon_M > 0$ denotes the maximum value of the neural approximation error ϵ. In our case, we take the neural networks inputs $X_{in} = [\widetilde{\xi}, \dot{\widetilde{\xi}}, \xi_r, \dot{\xi}_r, \ddot{\xi}_r]$.

Theorem 3.1. *Consider the quadrotor translational dynamics described in (12), or equivalently (16)-(19). If the control input and the adaptive weight update law are designed as*

$$u = \frac{1}{M}\left(ge_3 + \hat{f} + K_v\gamma\right), \tag{20}$$

$$\dot{\hat{W}} = AP(X_{in})\gamma^T, \tag{21}$$

where K_v is a positive constant and A is a positive-definite symmetric matrix of gains, then the speed tracking and position tracking can be guaranteed regardless of uncertain systematic parameters and disturbances.

Proof. Consider the following Lyapunov function candidate

$$V = \frac{1}{2}\gamma^T\gamma + \frac{1}{2}tr\left(\widetilde{W}^T A^{-1}\widetilde{W}\right), \tag{22}$$

where $\widetilde{W} = W^* - \hat{W}$ denotes the vector of weight errors, and A^{-1} is the adaptive gain. Differentiating (22) using (16) produces

$$\dot{V} = \gamma^T(-Mu + ge_3 + f) + tr(\widetilde{W}^T A^{-1}\dot{\widetilde{W}}). \tag{23}$$

From adaptive law (21), we can obtain that $\dot{\widetilde{W}} = -AP(X_{in})\gamma^T$. In view of (20), the Lyapunov derivative (23) becomes

$$\begin{aligned}\dot{V} &= \gamma^T(f - \hat{f} - K_v\gamma) + tr(\widetilde{W}^T A^{-1}\dot{\widetilde{W}}) \\ &= -\gamma^T K_v \gamma + tr\widetilde{W}^T(A^{-1}\dot{\widetilde{W}} + P\gamma^T) + \gamma^T\epsilon \\ &= -\gamma^T K_v\gamma + \gamma^T\epsilon, \end{aligned} \tag{24}$$

where $\|\gamma\| > \epsilon_M/K_v$ ensures $\dot{V} < 0$. Thus, by choosing appropriate value of K_v, we can obtain $\dot{V} < 0$. Summing up, V is positive definite and $\dot{V}$ is negative, so the tracking error will be uniformly ultimately bounded. □

Furthermore, the control signal T is u_3, and from (11), we can get two desired attitude angles which will be used as desired trajectory in rotational subsystem, that is

$$\begin{cases} \phi_r(t) = arcsin(u_1 sin\psi(t) - u_2 cos\psi(t)) \\ \theta_r(t) = arcsin((u_1 cos\psi(t) + u_2 sin\psi(t))/cos\phi_r(t)) \end{cases} \tag{25}$$

3.2. Integral SMC for Attitude Stabilization

In this section, a double-loop integral sliding mode controller is proposed to stabilize attitude angles in rotational subsystem. In traditional sliding mode control, it is hard to solve the derivatives of $M(\eta)$ in (9), because there is strong coupling between ϕ, θ and ψ. Thus, double-loop integral SMC is introduced to avoid the above problem, while integral function helps to guarantee system's stability and zero errors under disturbances.

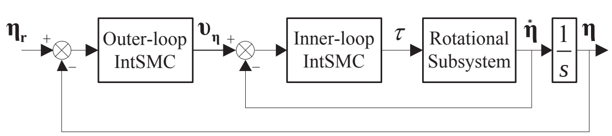

Figure 4. Double-loop integral sliding mode control.

The control diagram is given in Figure 4. We can see that outer-loop and inner-loop control angle position and angle velocity respectively. Add disturbance item $D_\eta = [D_{\eta 1}, D_{\eta 2}, D_{\eta 3}]^T$ into rotational model (9), and we can rewrite rotational model equation as

$$M(\eta)\ddot{\eta} + C(\eta, \dot{\eta})\dot{\eta} + D_\eta = \tau. \tag{26}$$

As for the control of attitude angles in outer loop, we define the integral sliding mode surface as

$$s_w = \widetilde{\eta} + k_w \int_0^t \widetilde{\eta} \mathrm{d}t, \tag{27}$$

where k_w is a positive constant and $\widetilde{\eta} = \eta_r - \eta$ is error vector of the aircraft attitude. Differentiating (27) produces

$$\dot{s}_w = \dot{\eta}_r - v_\eta + k_w \widetilde{\eta}, \tag{28}$$

where v_η represents the control inputs of outer-loop SMC, which can be designed using Lyapunov theory and can be achieved by inner-loop SMC [31].

As for the control of attitude angles' velocity in inner loop, we define the sliding mode surface as

$$s_n = \widetilde{v} + k_n \int_0^t \widetilde{v} \mathrm{d}t, \tag{29}$$

where k_n is a positive constant and $\widetilde{v} = v_\eta - \dot{\eta}$ is the error vector of angle velocity. According to (26), the differential form of (29) can be written as

$$\dot{s}_n = \dot{v}_\eta + M^{-1} C \dot{\eta} - M^{-1} \tau - M^{-1} D_\eta + k_n \widetilde{v}. \tag{30}$$

To achieve $v_\eta \to \dot{\eta}$, control law τ is designed for tracking the angle velocity .

Theorem 3.2. *In the outer-loop integral SMC controller, control law of v_η is designed as*

$$v_\eta = \dot{\eta}_r + k_w \widetilde{\eta} + \rho_w \mathrm{SGN}(s_w), \tag{31}$$

where ρ_w is a positive constant, which determines the convergence rate of attitude angles. The control law of inner-loop is designed as

$$\tau = M\dot{v}_\eta + C\dot{\eta} + \rho_n \mathrm{SGN}(s_n) + k_n M\widetilde{v}, \tag{32}$$

where ρ_n is a positive constant, which determines the convergence rate of attitude angles' velocity. By designing these two laws with appropriate feedback gains, we can ensure that the aircraft attitude position and velocity will achieve asymptotic tracking convergence even in the presence of disturbance.

Proof. Consider the following Lyapunov function

$$V_w = \frac{1}{2} s_w^T s_w. \tag{33}$$

From (28), the differential form of (33) is

$$\dot{V}_w = s_w^T(\dot{\eta}_r - v_\eta + k_\eta \widetilde{\eta}). \tag{34}$$

Substitute control law (31) into (34), resulting in

$$\begin{aligned} \dot{V}_w &= -\rho_w s_w^T \mathrm{SGN}(s_w) \\ &= -\rho_w \sum_{i=1}^{3} |s_{wi}| \\ &\leq 0. \end{aligned} \tag{35}$$

Thus, attitude angles errors will converge to zero along the desired integral sliding mode surface.

In the inner loop, we choose Lyapunov function

$$V_n = \frac{1}{2} s_n^T s_n. \tag{36}$$

According to (30) and control law (32), the differential form of (36) is given as follows

$$\begin{aligned} \dot{V}_n &= s_n^T(\dot{v}_\eta + M^{-1}C\dot{\eta} - M^{-1}\tau - M^{-1}D_\eta + k_n\widetilde{v}) \\ &= s_n^T M^{-1}(-\rho_n \mathrm{SGN}(s_n) - D_\eta) \\ &\leq -\lambda_{max}(M^{-1})|s_n|(\rho_n - \|D_\eta\|), \end{aligned} \tag{37}$$

with $\lambda_{max}(M^{-1})$ denoting the maximum eigenvalue of M^{-1}. Thus, if we take $\rho_n \geq \|D_\eta\|$, the Lyapunov equation $\dot{V}_n \leq 0$ can ensure that attitude angles' velocity errors will converge to zero along the above integral sliding mode surface. In practical applications, to avoid the chattering phenomenon, sigmoid functions are introduced to replace sign functions and they are $2/(1+exp(-x/500))-1$ and $2/(1+exp(-x/10))-1$ in outer loop and inner loop, respectively. □

4. Simulation Results

In this section, several simulation examples are given to illustrate the effectiveness of the proposed control strategy for path following problem. The parameters of the quadrotor aircraft used in the simulations are given in Table 1, which are chosen from the test [27]. Besides, simulations compare the control structure developed in this paper with traditional PD strategy and backstepping/nonlinear H_∞ to show the improvement. And all simulations have been executed considering external disturbances on the six DOF and system model uncertainties, while noise is introduced in the second example to indicate the robustness of the control method.

Table 1: Parameters of the quadrotor aircraft

Symbol	Value	Unit
m	0.74	kg
g	9.81	m/s^2
d	0.2	m
I_{xx}, I_{yy}	0.004	kgm^2
I_{zz}	0.0084	kgm^2

Example 4.1 In this example, the reference path used is a circle evolving

in the R^3 Cartesian space defined by

$$x_r = \frac{1}{2}cos(\frac{\pi t}{20}) \text{ m}, \;\; y_r = \frac{1}{2}sin(\frac{\pi t}{20}) \text{ m}$$
$$z_r = 3 - 2cos(\frac{\pi t}{20}) \text{ m}, \;\; \psi_r = sin(\frac{\pi t}{20}) \text{ rad}.$$

Sustained disturbances and parameters uncertainties have been imposed on the quadrotor to indicate the ability of anti-disturbance and robustness. Also the result is compared with PD/InitSMC control method. Suppose that the initial conditions of the aircraft are $\xi_0 = [0.45, 0.05, 0.45]^T$ m and $\eta_0 = [0.1, 0.1, 0.1]^T$ rad. The adaptive RBFNNs controller parameters are adjusted as $J = 7$, $c_i = [-1.5, -1, -0.5, 0, 0.5, 1, 1.5]$, $\sigma = 5$, $\Lambda = 3$, $A = 100$ and $K_v = 15$. And the sliding mode controller gains are tuned with the following values, $k_w = 100$, $\rho_w = 5$, $k_n = 20$ and $\rho_n = 25$.

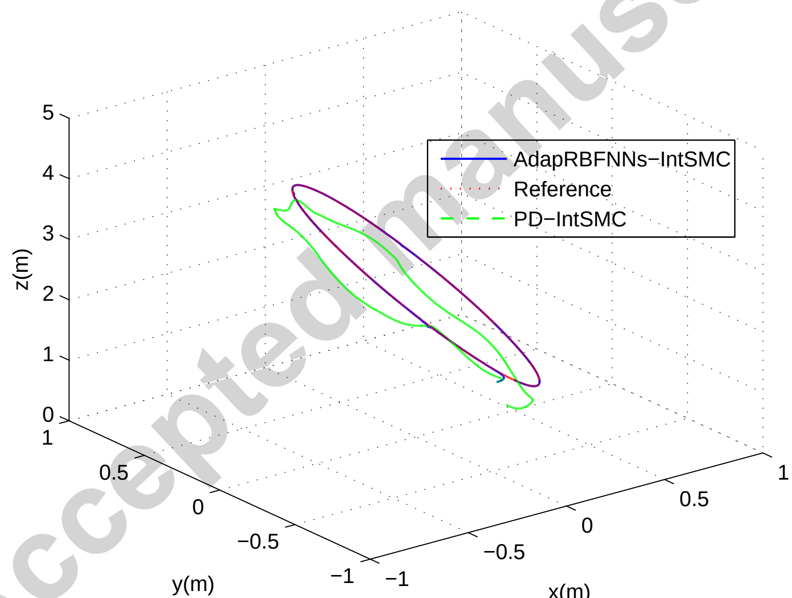

Figure 5. Path following.

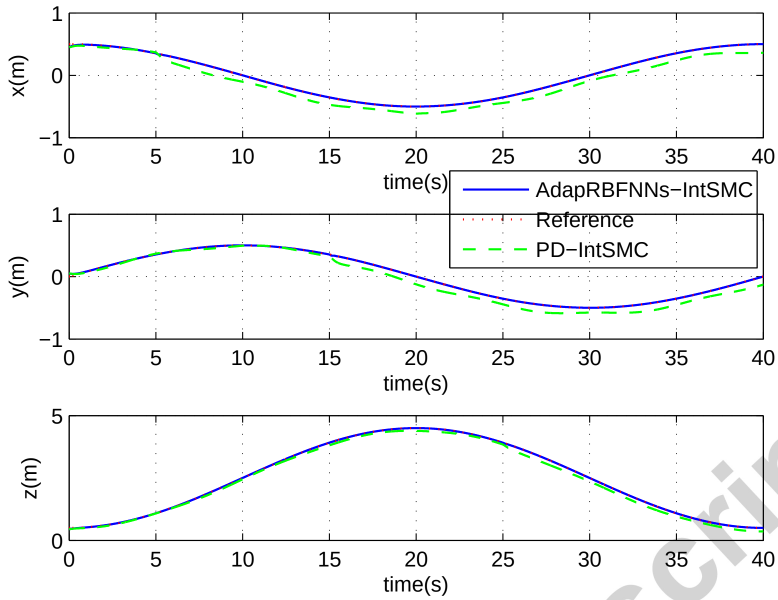

Figure 6. Position tracing.

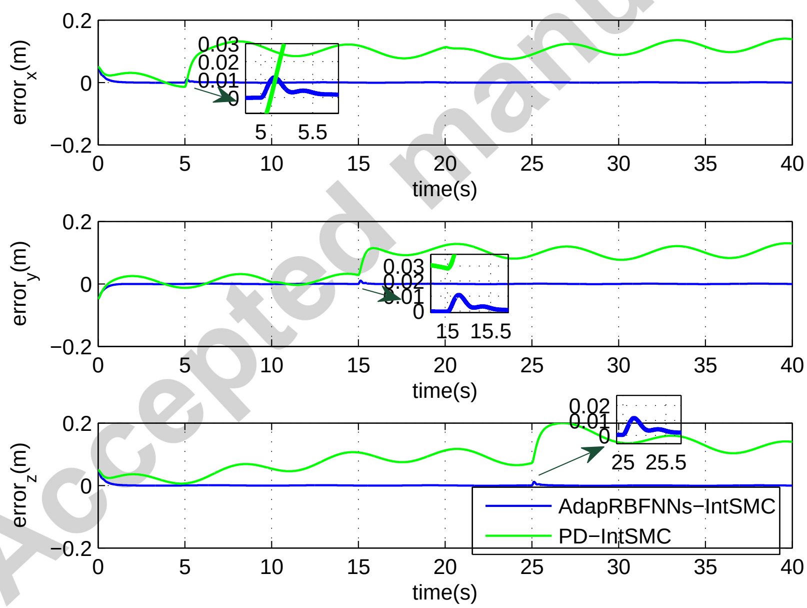

Figure 7. Position error.

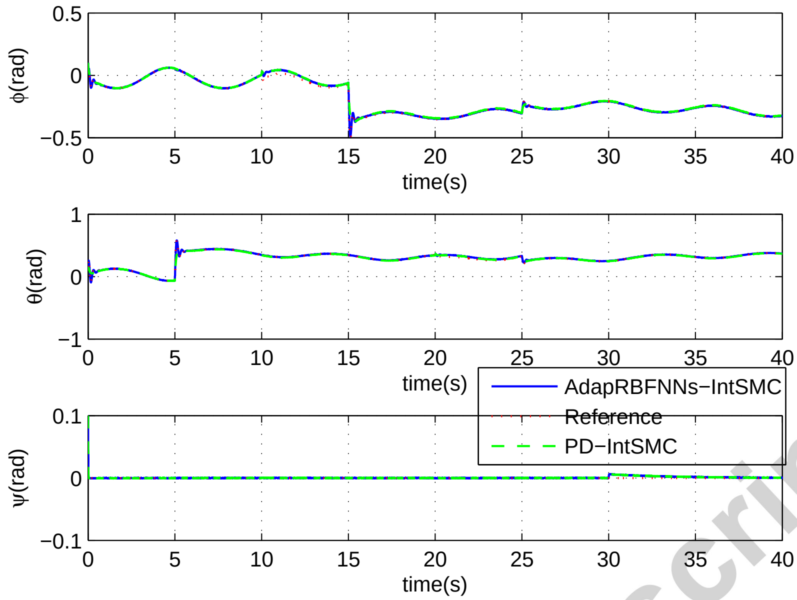

Figure 8. Orientation tracing.

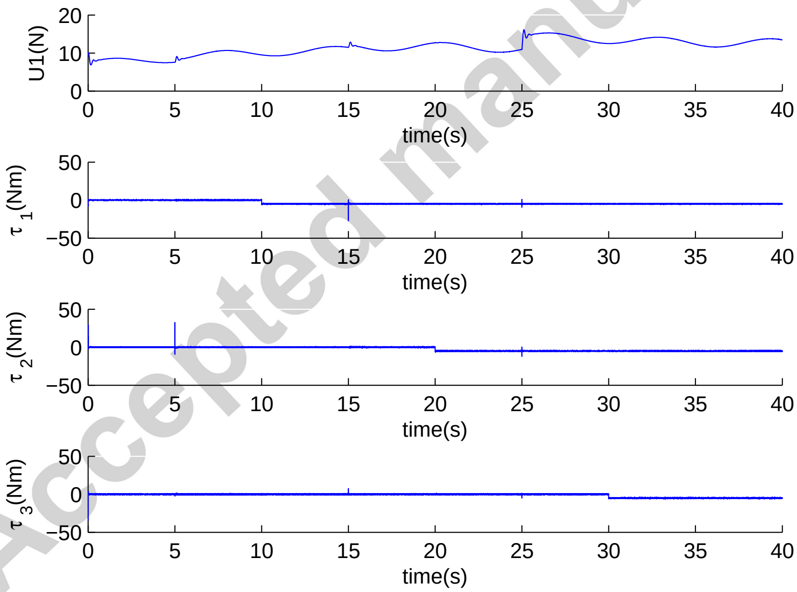

Figure 9. Control inputs.

External disturbances on the aerodynamic forces and moments are given as : $D_{\xi x} = 5$ N at $t = 5$ s; $D_{\xi y} = 5$ N at $t = 15$ s; $D_{\xi z} = 5$ N at $t = 25$ s;

$D_{\eta 1} = 5$ Nm at $t = 10$ s; $D_{\eta 2} = 5$ Nm at $t = 20$ s; $D_{\eta 3} = 5$ Nm at $t = 30$ s. Parameter uncertainties are defined as $\Lambda = \xi + \dot{\xi} + sin(t)$.

Simulation results of the path following and control inputs are shown in Figures 5-9, and performance is noticeable in these figures especially at the time when disturbances of forces and moments occur. It can be seen how, starting from an initial position far from the reference, the proposed control strategy is able to make the vehicle follow the reference trajectory in a small delay. Position tracing results in 3-D space and separate space are present in Figure 5 and Figure 6 respectively. Figure 7 shows the translational tracking errors, and it can be observed that translational tracking is well achieved, even if structural uncertainty is considered in the vehicle.

In contrast, simulation results using PD-IntSMC controller without adaptive RBFNNs compensation is considered, and the results are also presented in Figure 5-7. It can be seen the quadrotor leaves the predetermined trajectory when a disturbance is introduced, and it never reaches the reference trajectory again. Besides, the curve is affected when parameter uncertainties of Λ changed.

Figure 8 shows that inner integral sliding mode controller makes the vehicle track its rotational references trajectory when each degree of freedom is affected by the moment disturbances. The reference attitude angles of ϕ_r and θ_r generated by the translational controller varies with time, but the integral sliding mode controller achieves null steady-state error. Finally, four control inputs are presented in Figure 9, including three torque inputs and one force input. Due to the replacement of the sign function by the sigmoid function, the control inputs avoid the chattering problem so that the obtained input control signals are acceptable and physically realizable. From these figures, the designed controller succeeds in reaching the desired trajectory while disturbances and model uncertainty are well compensated.

Example 4.2 In order to evaluate the performance of the controller, another simulation with a stricter situation has been provided and some new results are shown and analyzed. This flight simulation has been carried out with a reference trajectory made up of a set of line stretches [32]. The noise applied to the translational and rotational subsystem is Gaussian noise with zero mean and standard deviation of 1 (Nm or N), which is given in Figure 10, in order to verify the noise immunity and robustness of this controller.

The values of the model parameters used for simulations are given in Table 1. External disturbances on the aerodynamic forces and moments are as same as those in Example 4.1. And the initial conditions of the helicopter are $\xi_0 = [-0.46, 0.46, 0.02]^T$ m and $\eta_0 = [0, 0, 0.1]^T$ rad.

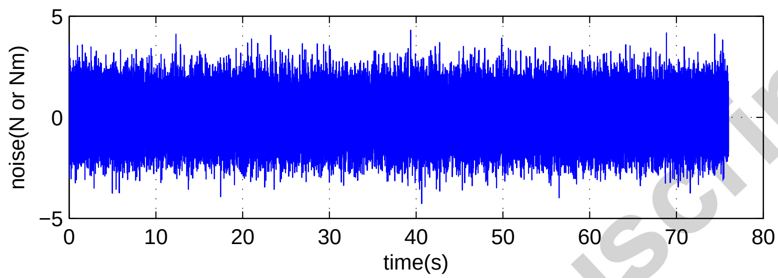

Figure 10. Gaussian noise.

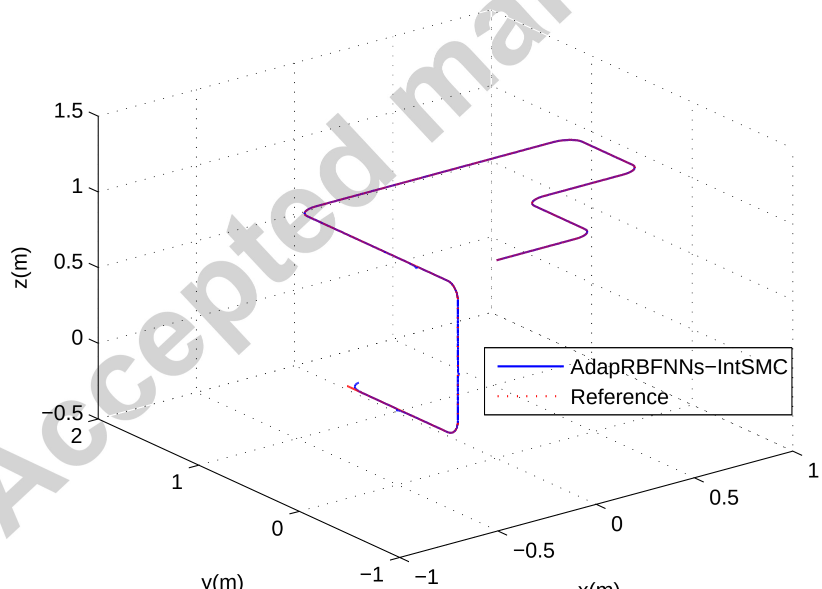

Figure 11. Path following.

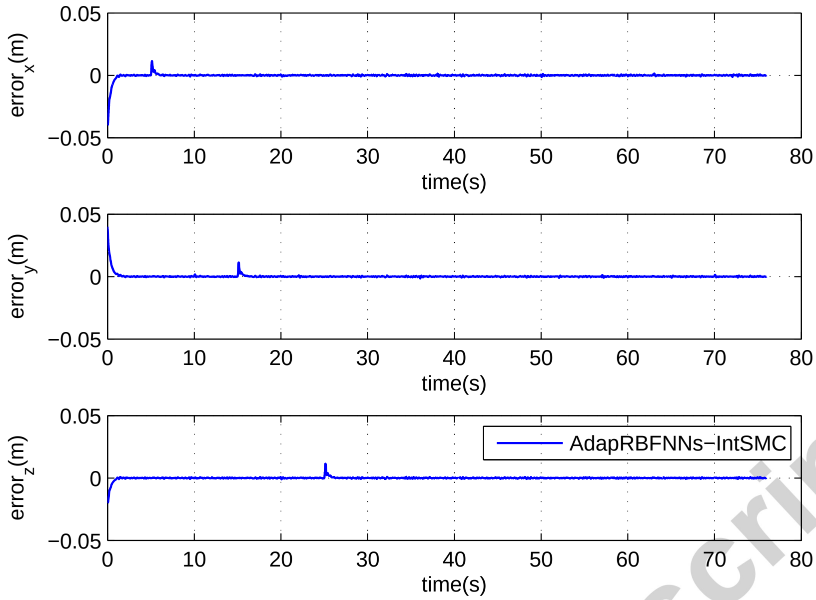

Figure 12. Position error.

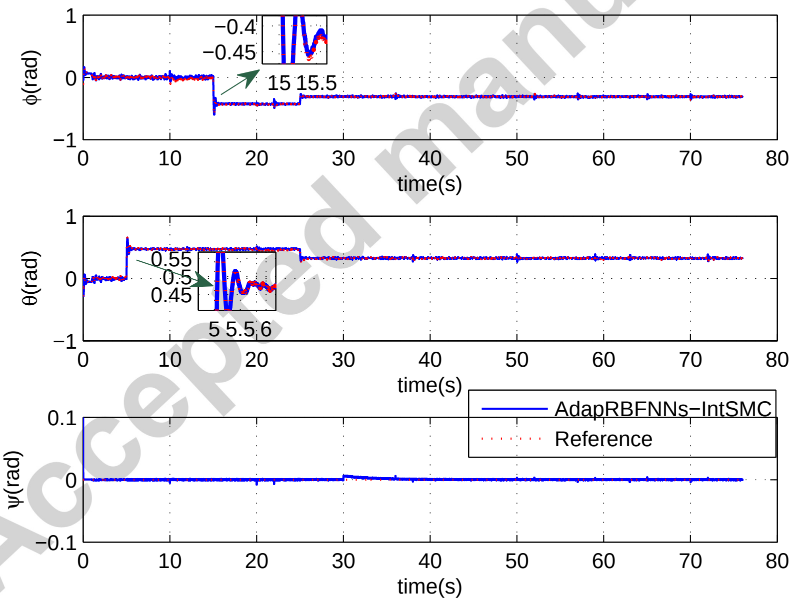

Figure 13. Attitude error.

Figures 11-13 show the simulation results of the proposed controller for the quadrotor in the presence of noise effect while considering Gaussian noise.

The noise with zero mean and standard deviation of 1 N and 1 Nm is injected at the x, y, z, ϕ, θ and ψ, respectively. Figure 11 shows the absolute position of the quadrotor during its flight, indicating that the aerodynamic force and moment disturbances are introduced, but the assigned navigational task is successfully achieved and the reference trajectory is tracked with high accuracy under Gaussian noise. Figure 12 represents the position tracking results, from which we can see a well good tracking of the desired translational trajectory, and the controller is able to reject the noise effect showing the robustness of the proposed approach and the stability of the closed loop dynamics. We can also notice in Figure 13 a same high performance in attitude tracking since the attitude errors under noise are much less than those under equal-amplitude disturbances. These figures show that the proposed controller presents a robust path following when irregular noise is applied to the system.

Example 4.3 In this example, simulation results have been obtained with a vertical helix reference trajectory. Initial conditions and system parameters are set appropriately in order to compare the simulation results with [33]. For this path, the helicopter starts at the initial position $\xi_0 = [0.5, 0, 1.0]^T$ m and $\eta_0 = [0, 0, 0.5]^T$ rad, with disturbances of force and moment. In this simulation, results attained by the adaptive RBFNNs/IntSMC strategy are compared with the results achieved by the backstepping/nonlinear H_∞ method.

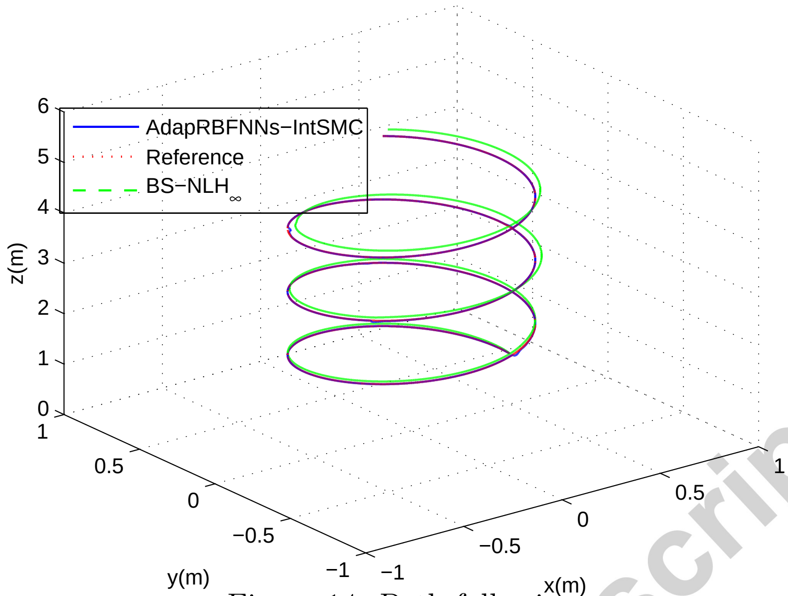

Figure 14. Path following.

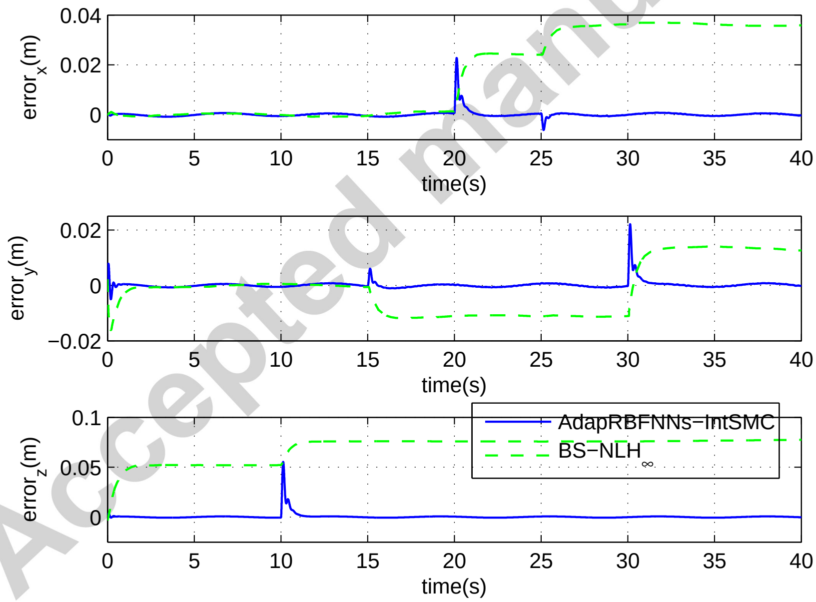

Figure 15. Position error.

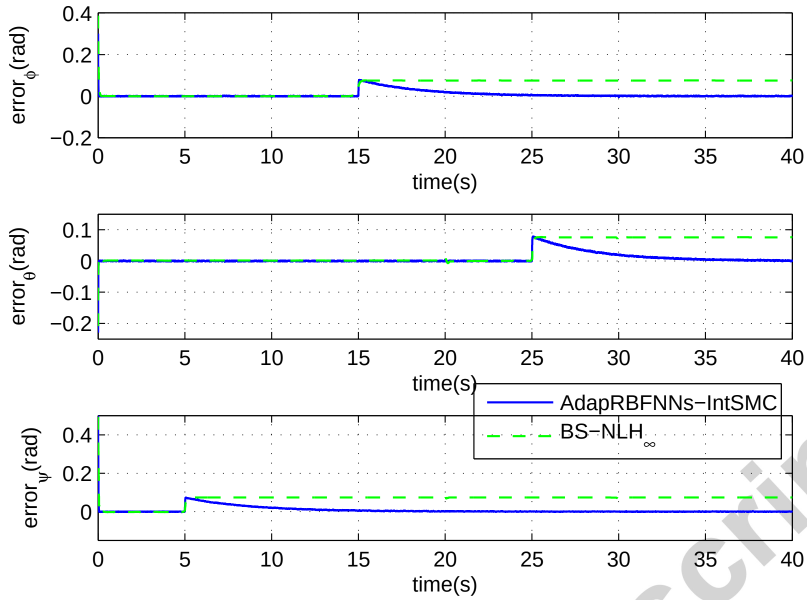

Figure 16. Attitude error.

The simulation results are given in Figures 14-16. These figures illustrate that the proposed control strategy and the BS/NLH$_\infty$ approach both present a robust path tracking when parameter uncertainties are imposed on the quadrotor helicopter model. However, the improvement generated by the use of the integral action is clearly pointed out. In the BS/NLH$_\infty$ case, the vehicle leaves the reference trajectory when the disturbances are introduced, and it never reaches the reference trajectory again. In addition, Figures 15 and 16 show that the helicopter degrees of freedom can not obtain a null steady-state when no integral term is considered in the controllers synthesis. Besides, when the control strategy proposed in this paper is compared with the integral BS/NLH$_\infty$ control presented in [34], it can be clearly observed that controller proposed in this paper reduces the convergence time under same circumstance including same disturbances and system dynamics, and the results of IntBS/NLH$_\infty$ can be found in [34]. Thus, according to results in this simulation, controller proposed in this paper obtains faster convergence rate by adaptive RBFNNs control and null steady-error by integral sliding mode control.

5. Conclusions

In this paper, a constructive hierarchical controller composed of adaptive RBFNNs and double-loop integral SMC is developed to solve the path following problem for a quadrotor helicopter under consideration of external disturbances acting on all degrees of freedom. An adaptive radical biased neural networks controller for the translational movements has been proposed, and achieves a good and smooth performance in tracking the desired trajectory. The tracking error is uniformly ultimately bounded and the size of the ultimate bound can be arbitrarily reduced by tuning control parameters. Besides, compensation ability of this controller helps reject sustained disturbances and parametric uncertainties that affect the translational motion.

On the other hand, double-loop integral sliding mode controller keeps the aircraft following the desired attitude commands, and the use of the integral action for state errors makes aircrafts able to reject sustained disturbances and achieve null steady-error. Also, sigmoid functions are introduced to alleviate the chattering problem such that the control signals become more practical.

The robustness, the smoothness and the nonlinear function approximation feature of the proposed control strategy have been corroborated by simulations, where parametric uncertainties and sustained disturbances have been taken into account. Tracking error comparisons between the proposed control strategy and three other controllers have been carried out to demonstrate that faster time response and null steady-error can be achieved by the proposed adaptive RBFNNs/IntSMC control strategy. And the simulation with Gaussian noise is conducted to illustrate the robustness of the this controller.

Future research is to apply and validate this novel control method in real applications. The quadrotor aircraft system shown in Figure 1 is being built, which includes an MPU-6050 sensor to obtain the attitude angles and a Kinect camera to calculate the position of the quadrotor via image location. Based on these signals and once the real physical parameters of our platform are attained by identification methods, we can apply the whole control strategy proposed in this paper to real-time experiments.

Acknowledgement

The authors would like to thank National Natural Science Foundation of China for funding this work under grants 61433016 and 61573134.

References

[1] M. Bosnak, D. Matko, S. Blazic, Quadrocopter control using an on-board video system with off-board processing, Robotics & Autonomous Systems 60 (4) (2012) 657–667.

[2] D. Maravall, J. de Lope, J. P. Fuentes, Vision-based anticipatory controller for the autonomous navigation of an uav using artificial neural networks, Neurocomputing 151 (2015) 101–107.

[3] M. A. R. Ai-Omari, M. A. Jaradat, M. Jarrah, Integrated simulation platform for indoor quadrotor applications, in: Mechatronics and its Applications (ISMA), 2013 9th International Symposium on, 2013, pp. 1–6.

[4] M. Elfeky, M. Elshafei, A. W. A. Saif, M. F. Al-Malki, Quadrotor with tiltable rotors for manned applications, in: Multi-Conference on Systems, Signals & Devices (SSD), 2014 11th International, 2014, pp. 1–5.

[5] I. Fantoni, R. Lozano, Non-Linear Control for Underactuated Mechanical Systems, Springer-Verlag New York, Inc., 2001.

[6] B. Erginer, E. Altuğ, Modeling and pd control of a quadrotor vtol vehicle, in: Intelligent Vehicles Symposium, 2007 IEEE, IEEE, 2007, pp. 894–899.

[7] S. Bouabdallah, A. Noth, R. Siegwart, Pid vs lq control techniques applied to an indoor micro quadrotor, in: Intelligent Robots and Systems, 2004.(IROS 2004). Proceedings. 2004 IEEE/RSJ International Conference on, Vol. 3, IEEE, 2004, pp. 2451–2456.

[8] A. Tayebi, S. Mcgilvray, Attitude stabilization of a vtol quadrotor aircraft, IEEE Transactions on Control Systems Technology 14 (3) (2006) 562–571.

[9] A. Das, F. Lewis, K. Subbarao, Backstepping approach for controlling a quadrotor using lagrange form dynamics, Journal of Intelligent & Robotic Systems 56 (1-2) (2009) 127–151.

[10] K. Alexis, G. Nikolakopoulos, A. Tzes, Switching model predictive attitude control for a quadrotor helicopter subject to atmospheric disturbances, Control Engineering Practice 19 (10) (2011) 1195–1207.

[11] J. Shin, H. J. Kim, S. Park, Y. Kim, Model predictive flight control using adaptive support vector regression, Neurocomputing 73 (4) (2010) 1031–1037.

[12] G. V. Raffo, M. G. Ortega, F. R. Rubio, Path tracking of a uav via an underactuated control strategy, European Journal of Control 17 (2) (2011) 194–213.

[13] F. K. Yeh, Attitude controller design of mini-unmanned aerial vehicles using fuzzy sliding-mode control degraded by white noise interference, Control Theory & Applications, IET 6 (9) (2012) 1205–1212.

[14] N. Guenard, T. Hamel, R. Mahony, A practical visual servo control for an unmanned aerial vehicle, IEEE Transactions on Robotics 24 (2) (2008) 331–340.

[15] L. Taeyoung, L. Melvin, M. N. Harris, Nonlinear robust tracking control of a quadrotor uav on se(3), Asian Journal of Control 15 (2) (2013) 391–408.

[16] M. Chen, Y. Zhou, W. W. Guo, Robust tracking control for uncertain mimo nonlinear systems with input saturation using rwnndo, Neurocomputing 144 (2014) 436–447.

[17] L. Derafa, A. Benallegue, L. Fridman, Super twisting control algorithm for the attitude tracking of a four rotors uav, Journal of the Franklin Institute 349 (2) (2012) 685–699.

[18] C. Nicol, C. Macnab, A. Ramirez-Serrano, Robust adaptive control of a quadrotor helicopter, Mechatronics 21 (6) (2011) 927–938.

[19] C. A., T. D., Z. Y.M., J. C., R. C.A., Active fault-tolerant control system design with trajectory re-planning against actuator faults and saturation: Application to a quadrotor unmanned aerial vehicle, International Journal of Adaptive Control & Signal Processing 29 (1) (2015) 1–23.

[20] Y. Chen, J. Yu, X. Su, G. Luo, Path planning for multi-uav formation, Journal of Intelligent & Robotic Systems 77 (1) (2015) 229–246.

[21] H. Ramirez-Rodriguez, V. Parra-Vega, A. Sanchez-Orta, O. Garcia-Salazar, Robust backstepping control based on integral sliding modes for tracking of quadrotors, Journal of Intelligent & Robotic Systems 73 (1-4) (2014) 51–66.

[22] R. Skjetne, T. Fossen, et al., On integral control in backstepping: Analysis of different techniques, in: American Control Conference, 2004. Proceedings of the 2004, Vol. 2, IEEE, 2004, pp. 1899–1904.

[23] L. Yu, S. Fei, X. Li, Robust adaptive neural tracking control for a class of switched affine nonlinear systems, Neurocomputing 73 (10-12) (2010) 2274–2279.

[24] T. Li, R. Li, D. Wang, Adaptive neural control of nonlinear mimo systems with unknown time delays, Neurocomputing 78 (1) (2012) 83–88.

[25] Y. Niu, D. W. Ho, J. Lam, Robust integral sliding mode control for uncertain stochastic systems with time-varying delay, Automatica 41 (5) (2005) 873–880.

[26] R. Olfati-Saber, A. Megretski, Nonlinear control of underactuated mechanical systems with application to robotics and aerospace vehicles, Massachusetts Institute of Technology.

[27] G. V. Raffo, M. G. Ortega, F. R. Rubio, An integral predictive/nonlinear h_∞ control structure for a quadrotor helicopter, Automatica 46 (2010) 29–39.

[28] N. Sadati, R. Ghadami, Adaptive multi-model sliding mode control of robotic manipulators using soft computing, Neurocomputing 71 (2008) 2702–2710.

[29] Q. Zhu, T. Zhang, S. Fei, Adaptive tracking control for input delayed mimo nonlinear systems, Neurocomputing 74 (1) (2010) 472–480.

[30] Y. Cui, H. Zhang, Y. Wang, Z. Zhang, Adaptive neural dynamic surface control for a class of uncertain nonlinear systems with disturbances, Neurocomputing 165 (2015) 152–158.

[31] M. O. Efe, Integral sliding mode control of a quadrotor with fractional order reaching dynamics, Transactions of the Institute of Measurement & Control 33 (8) (2011) 985–1003.

[32] M. R. Mokhtari, B. Cherki, A new robust control for minirotorcraft unmanned aerial vehicles, ISA transactions 56 (2015) 86–101.

[33] G. V. Raffo, M. G. Ortega, F. R. Rubio, Backstepping/nonlinear h control for path tracking of a quadrotor unmanned aerial vehicle, in: American Control Conference, 2008, IEEE, 2008, pp. 3356–3361.

[34] G. V. Raffo, M. G. Ortega, F. R. Rubio, Robust nonlinear control for path tracking of a quad-rotor helicopter, Asian Journal of Control 17 (1) (2015) 142–156.